2013

CANNABINOIDS DELTA-9-TETRAHYDROCANNABINOL (THC) AND CP55,940 ABLATE SPECIFIC CHEMOKINE AND CYTOKINE INFLAMMATORY RESPONSE IN BV-2 MOUSE MICROGLIAL CELLS ACTIVATED WITH HIV-1 PRO-INFLAMMATORY PROTEIN TAT

Rebecca Maddux
Virginia Commonwealth University

School of Medicine
Virginia Commonwealth University

This is to certify that the thesis prepared by Rebecca Anne Maddux entitled CANNABINOIDS DELTA-9-TETRAHYDROCANNABINOL (THC) AND CP55,940 ABLATE SPECIFIC CHEMOKINE AND CYTOKINE INFLAMMATORY RESPONSE IN BV-2 MOUSE MICROGLIAL CELLS ACTIVATED WITH HIV-1 PRO-INFLAMMATORY PROTEIN TAT has been approved by his or her committee as satisfactory completion of the thesis requirement for the degree of Master of Science in Microbiology and Immunology

Guy A. Cabral, Ph.D., Director of Thesis

Cynthia Cornelissen, Ph.D., Virginia Commonwealth University School of Medicine

Kurt Hauser, Ph.D., Virginia Commonwealth University School of Medicine

Dennis Ohman, Ph.D., Chair, Department of Microbiology and Immunology

Jerome F. Strauss, III, MD., Ph.D., Dean, School of Medicine

Dr. F. Douglas Boudinot, Dean of the Graduate School

June 25, 2013

CANNABINOIDS DELTA-9-TETRAHYDROCANNABINOL (THC) AND CP55,940 ABLATE SPECIFIC CHEMOKINE AND CYTOKINE INFLAMMATORY RESPONSE IN BV-2 MOUSE MICROGLIAL CELLS ACTIVATED WITH HIV-1 PRO-INFLAMMATORY PROTEIN TAT

A Thesis submitted in partial fulfillment of the requirements for the degree of Master of Science at Virginia Commonwealth University.

by

REBECCA ANNE MADDUX
Bachelor of Science, University of Virginia, 2010

Director: DR. GUY A. CABRAL, PH.D.
PROFESSOR, DEPARTMENT OF MICROBIOLOGY AND IMMUNOLOGY

Virginia Commonwealth University
Richmond, Virginia
August, 2013

Acknowledgement

I would like to first express my sincere gratitude to my advisor, Dr. Guy Cabral, for creating such an enjoyable learning environment and for his endless support, expert guidance, and assistance throughout this process. This thesis would not have been possible if it had not been for his continued commitment to my success as a Master's student. It has truly been a privilege to work alongside him this past year. I would also like to thank Dr. Francine Marciano-Cabral for her continued support and encouragement. Together, their warmth and kindness has provided me with such a positive laboratory experience and has been instrumental in my success and in the completion of this project.

In addition, I would also like to thank the members of my committee, Dr. Cynthia Cornelissen and Dr. Kurt Hauser. I truly appreciate all of the time they dedicated to helping me complete my thesis as well as the valuable insight and help with which they provided me.

Also, I would like to thank Dr. Gabriela Ferreira for her guidance and assistance. She has been an excellent teacher, and I owe a great amount of my graduate success to her. I would like to thank my fellow laboratory members and colleagues including Dr. Melissa Jamerson, Dr. Erinn Raborn, Hong Park, and Johnathan Drevik for their continued support. Finally, I would like to thank my parents, Robert and Sharry

Maddux, and my sister, Jessica Maddux for their unconditional love and support. This would not have been possible without them.

Table of Contents

List of Tables

Page

List of Figures

Page

List of Abbreviations

2-D	Two-Dimensional
ADC	AIDS Dementia Complex
AIDS	Auto-Immune Deficiency Syndrome
BBB	Blood-Brain Barrier
BSA	Bovine Albumin Serum
CB1	Cannabinoid Receptor Type 1
CB2	Cannabinoid Receptor Type 2
CDC	Center for Disease Control and Prevention
cDNA	Complementary DNA
CNS	Central Nervous System
DNA	Deoxyribonucleic Acid
FAT	Factor Acetyltransferase
HAART	Highly-Active Anti-retroviral Therapy
HAND	HIV-Associated Neurocognitive Disorder
HAD	HIV-Associated Dementia
HAT	Histone Acetyltransferase
HIV	Human Immunodeficiency Virus
HIVE	HIV-Associated encephalitis
LPS	Lipopolysaccharide
MAP	Mitogen-Activated Protein
MCMD	Minor Cognitive Motor Disorder
mRNA	Messenger RNA
MTT	3-(4,5-dimethyl-2-thiazolyl)-2,5-diphenyl-2H-tetrazolium bromide
NF-kappaB	Nuclear Factor-KappaB
PAGE	Polyacrylamide Gel Electrophoresis
PCR	Polymerase Chain Reaction
PM	Primary Microglia

Tat	Transactivating protein
THC	Δ^9-tetrahydrocannabinol
TNF	Tumor Necrosis Factor
RNA	Ribonucleic Acid
SDS	Sodium Dodecyl Sulfate

Abstract

CANNABINOIDS DELTA-9-TETRAHYDROCANNABINOL (THC) AND CP55,940 ABLATE SPECIFIC CHEMOKINE AND CYTOKINE INFLAMMATORY RESPONSE IN BV-2 MOUSE MICROGLIAL CELLS ACTIVATED WITH HIV-1 PRO-INFLAMMATORY PROTEIN TAT

By Rebecca Anne Maddux, M.S.

A Thesis submitted in partial fulfillment of the requirements for the degree of Master of Science at Virginia Commonwealth University.

Virginia Commonwealth University, 2013.

Major Director: Dr. Guy A. Cabral, PhD.
Professor, Department of Microbiology and Immunology

Despite the widespread use of Highly Active Anti-retroviral Therapy (HAART) to combat Human Immunodeficiency Virus (HIV), the causative agent of acquired immunodeficiency syndrome (AIDS), HIV-Associated Neurocognitive Disorders (HANDs) still remain a dire issue. HIV can enter the brain through infected monocytes and infect microglia, the resident macrophages within that compartment. Due to its pro-

inflammatory properties, HIV regulatory protein Tat (Transactivating protein) may play a role in the progression of neurocognitive disorders.

The aim of this project was to determine whether the select cannabinoids THC and CP55,940 could ablate the inflammatory response on BV-2 mouse microglia cells caused by Tat. Within the constraints of the experiment, no major effects of cannabinoid treatment were observed at the level of the proteome as tested by two-dimensional gel electrophoresis . In contrast, these cannabinoids ablated the inflammatory response caused by the HIV protein Tat at the level of the secretome and at the level of gene expression. These collective observations suggest that select cannabinoids have the potential to down-regulate the elicitation of proinflammatory gene products that are engendered by the HIV protein Tat. Furthermore, the results suggest a potential for cannabinoid agonists at cannabinoid receptors to serve as adjunct ablative agents in the treatment of HIV-associated neuropathological processes.

Introduction

Human Immunodeficiency Virus

The Human Immunodeficiency Virus (HIV) is an enveloped lentivirus, a member of the retrovirus family, that is the causative agent of acquired immunodeficiency syndrome (AIDS). According to the Centers for Disease Control and Prevention (CDC, 2010), approximately 1,148,200 people aged 13 and older are living with HIV infection in the United States of America. Of the infected population, approximately 1 in 5, or 20%, are unaware that they are infected (CDC). HIV has the ability to infect many cell types, principally CD4+ T cells and macrophages, with macrophages typically being the earlier cellular target (Carter and Ehrlich, 2008). Eventually, HIV infection of immune cells leads to the loss of cell-mediated immunity, causing the body to become more susceptible to opportunistic infections. In addition, HIV is able to cross the blood-brain barrier (BBB) via infected macrophages and enter the central nervous system (CNS) early in HIV infection. (McArthur, 2005).

HIV-Associated Encephalitis

Due to the physical and cellular barrier provided by the BBB, the majority of pathogens cannot penetrate and infect the brain (Reviewed by Chiara, 2012). Among the

few viruses that can enter the brain and cause encephalitis, such as herpes simplex virus type 1(HSV-1), cytomegalovirus (CMV), Varicella zoster, and Epstein-Barr virus, HIV-1 is the leading cause of dementia (Almeida, 2005, Wang, 2006). The most widely accepted theory of how lentiviruses such as HIV enter into the CNS is through the "Trojan Horse" mechanism (Peluso, 1985). In this mechanism, the virus is trafficked into the brain by infected monocytes that can cross the BBB and then release the virus into the CNS. It has been reported that HIV can enter the brain as early as 15 days after systemic infection (Davis, 1992). While neurocognitive effects are rare in the asymptomatic phase of HIV infection, they can progress in the later stages of the disease (McArthur *et al*, 1989). According to a review by Ghafouri et al (2006), although there is a wide range of symptoms, neurological impairments affect approximately 60% of HIV-infected patients. The progressive cognitive disorders associated with HIV were originally described by Navia et al. (1986) under the name "AIDS dementia complex" (ADC). Since then, a collection of names, including HIV-associated dementia (HAD), HIV-Associated Neurocognitive Disorders (HANDs), and HIV encephalitis (HIVE) have been used to describe various cognitive disorders associated with HIV.

As discussed by Ghafouri et al, (2006) highly active anti-retroviral therapy (HAART) has substantially reduced, though not eliminated, the percentage of the AIDS population that suffers from HAD. Since HAART began in 1995, however, a more mild form of CNS dysfunction, called minor cognitive motor disorder (MCMD) has become increasingly common in HIV patients. HAART, however, is not designed to target the inflammatory cascade underlying HAD and MCMD, and in addition, protease inhibitors

cannot cross the BBB. Furthermore, HIV-1 RNA levels in the CNS do not always correlate with the degree of neurologic impairment in the course of HIV-associated dementia (Bossi et al., 1998). Thus, with the increase of use of HAART and as HIV-positive patients begin to live longer with the disease, it is anticipated that the range and prevalence of HIV-associated neurological diseases will increase, so treatment of HIV-1 associated dementia remains a dire issue.

Transactivating Protein (Tat)

It has been suggested that soluble mediators, such as the HIV pro-inflammatory protein Tat (transactivating protein), play a role in progression of the disease and could be responsible for encephalitis in the brain in the absence of abundant infection of the HIV virus itself (D'Aversa, 2004). First demonstrated by Dayton et al. (1986), HIV Tat is a viral regulatory protein that is necessary for both viral transcription and replication. As reviewed by Pugliesi et al. (2006), Tat has several subtypes that consist of between 72 and 101 amino acids depending on specific mRNA splicing. Tat protein is encoded by 2 exons. Exon 1 encodes amino acids 1-72, while exon 2 can encode either amino acids 73-86 or amino acids 73-101. Tat acts by accumulating in the nucleus of infected cells and enhancing viral transcription by binding to specific sequences of the Transactivation Response Element (TAR). Through this interaction, Tat recruits a myriad of transcriptional complexes, including histone acetyltransferases (HATs) and factor acetyltransferases (FATs), which promote elongation of viral RNA transcription (Brigati et al 2006). Tat also can activate transcription factor Nuclear Factor-kappaB (NF-kB)

(DeMarchi, 1996). Tat also activates glial cells to produce cytokines and chemokines such as Tumor Necrosis Factor (TNF)-α (Chen, 1997).

While Tat can remain intracellular, it also can act as a pleiotropic exogenous factor, and can regulate cellular activities related to survival, growth, inflammation, and angiogenesis (Brigati et al., 2006, Chang et al. 1995). Tat has been detected both within the CNS (Hudson et al., 2000) and in the serum of patients infected with HIV (Westendorp et al., 1995). Tat released from infected macrophages and microglia can enter neighboring neurons where it has pro-apoptotic potential (Ramirez, 2001). Extracellular Tat also activates neighboring cells, triggering even more production of chemokines and cytokines (D'Alversa, 2004). HIV-1 Tat protein also upregulates inflammatory mediators and induces monocyte invasion into the brain (Pu, 2003).

Microglia

There are five main cells types in the brain that are susceptible to the action of HIV infection: astrocytes, oligodendrocytes, neurons, perivascular macrophages, and microglia (Gonzalex-Scarano & Martin-Garcia, 2005). Microglia cells are one of three main glial cell types in the CNS. It is generally believed that during embryonic development, monocytes in the bloodstream are able to enter the brain and can then separate into resident microglial cells. Once activated, microglial cells act as immune stimulators and can lead to neurodegeneration, and in turn a variety of neurological disorders caused by neuroinflammation. Microglia can act as viral reservoirs that secrete inflammatory mediators and toxins that can affect the surrounding environment in the

central nervous system. Macrophages and microglia play a crucial role in HANDs and HIVE because they constitute the majority of cells infected with HIV-1 within the CNS (Lipton and Gendelman, 1995). Once a patient is infected with HIV-1, circulating monocytes in the body can migrate to the brain, where other cell types, including microglia, can be infected.

Because primary microglia cultures have many limitations for *in vitro* use, such as limited proliferation capacity and difficulty of obtaining pure cultures, microglial cell lines have become widely popular as experimental models, including both human and murine models. The murine BV-2 microglia cell line was produced through immortalization by a v-raf/v-myc oncogene carrying J2 retrovirus, (Blasi et al., 1990) and often is used as a substitute for primary microglia (PM) for *in vitro* experimentation. When activated by bacterial lipopolysaccharide (LPS), BV-2 cells elicit an overall response pattern of inflammatory genes that parallels that of primary microglial cells (PMs) (Henn, 2009). In addition, BV-2 cells behave similarly to PMs in assays examining Mitogen-Activated Protein (MAP) kinase signaling (Lund et al. 2005).

Cannabinoids and Cannabinoid Receptors

Originally isolated from the marijuana plant *Cannabis sativa,* exogenous cannabinoids represent a group of pharmacological compounds that have a wide array physiological and psychotropic effects on humans. Δ^9-tetrahydrocannabinol (THC), the major active ingredient of cannabis, was first isolated from hashish in 1964 (Gaoni and Mechoulam, 1964). In addition to its drug abuse potential, THC is responsible for a

multiplicity of effects in the CNS, including alterations in mood, perception, cognition, and memory (Dewey, 1986). As reviewed by Cabral and Pettit (1998), THC also has immunosuppressive properties that can decrease host defense in both guinea pigs and murine models to a variety of bacterial and viral infections.

Presently, two cannabinoid receptors (CB1 and CB2) have been discovered. CB1 was first isolated and cloned from rat cDNA (Matsuda, 1990), and CB2 was cloned shortly after from a human promyelocytic cDNA library (Munro, 1993). While both receptors are coupled to G-Proteins, CB1 is very abundant in the CNS, reaching high densities in the cerebellum, basal ganglia, hippocampus, and cortex (Pertwee, 1997). On the other hand, CB2 is found primarily in immune cells (Munro, 1993) and appears to play a major role in immune modulation (reviewed by Cabral and Dove Pettit, 1998) by regulating immune cell migration and cytokine release (reviewed by Cabral and Staab, 2005). Both the CB1 and CB2 receptors inhibit adenylyl cyclase and activate MAP kinase signaling (Howlett, 2005). Due to its location in the brain, activation of CB1 can affect memory and cognition processes and alter control of motor function (Pertwee, 2004). Microglia, the main cells in the CNS targeted by HIV, express the CB2 during CNS inflammation in models associated with HIV infection (Benito et al, 2005).

There are several receptor agonists that bind to CB1 and CB2, including THC and CP55940. The discovery that exogenous cannabinoids could alter function through the cannabinoid receptors implied the existence of an endogenous cannabinoid system (the endocannabinoids). As reviewed by Pertwee (2006), the distribution pattern of CB1 within

the CNS is consistent with those areas that are associated with the major psychotropic effects of THC.

Rationale and Objectives

Because neuroinflammation and the associated neurocognitive disorders remain a major concern with HIV-positive individuals and studies have shown that Tat has pro-inflammatory properties, the goal of this investigation was to assess the potential of select cannabinoids to ablate the microglial inflammatory response to HIV protein Tat. Microglial cells, specifically BV-2 mouse cells, were the focus of study since they represent the most HIV replication-competent cell population in the brain and the major reservoir of HIV in the CNS. The cannabinoids used in the study were THC (a partial agonist at cannabinoid receptors) and CP55,940 (a full agonist at cannabinoid receptors), which have both been previously known for their anti-inflammatory properties. THC was included in the study specifically because of its drug abuse implications in smoked marijuana and to assess whether, at least *in vitro*, it exacerbated the microglial immune response to Tat.

In order to address this goal, first, *in vitro* models of mouse microglial cells were established and proven to be viable following treatment with Tat, THC, and CP55940. Second, different protein profiles between different treatment groups were assessed using a high-resolution two-dimensional gel proteomics approach. Finally, a limited assessment of the secretome was undertaken through analysis of levels of cytokines and chemokines and their cognate mRNA species at the gene expression level. The collective results indicated

that THC and CP55940 ablated the inflammatory response of BV-2 mouse microglia-like cells exposed to exogenously-introduced Tat primarily by downregulating the levels of pro-inflammatory cytokines and chemokines.

Materials and Methods

Cells

The murine BV-2 cell line, produced through immortalization by a v-raf/v-myc oncogene carrying J2 retrovirus (Blasi et al., 1990), was obtained from Dr. Michael McKinley (Mayo Clinic, Jacksonville, FL). Cell cultures were maintained at 37°C with 5% CO_2 in ventilated T-175 flasks in complete Dulbecco's Modified Eagle's Medium (DMEM) (Mediatech, Herndon, VA) supplemented with 1% each of L-glutamine, non-essential amino acids, and MEM vitamins, 0.01M HEPES buffer, penicillin (100 IU/ml)/streptomycin, (100 μg/ml)/amphotericin B (0.25 μg/ml) and 10% heat-inactivated fetal bovine serum (HI-FBS). For experiments, because Tat attached to plastic, special low-retention microfuge tubes (Thermo Fisher Scientific, Waltham, MA) and low-binding pipette tips (VWR, West Chester, PA) were used. Confluent BV-2 cells were detached from culture flasks using a cell scraper (BC Falcon, Franklin Lakes, NJ) and were seeded at a density of 1 x 10^6 cells.

Drugs

The partial CB1R/CB2R agonist Delta-9-tetrahydrocannabinol,THC (CB1R Ki = 40.7 nM; CB2R Ki = 36.4 nM), and the full CB1R/CB2R agonist CP55940 (CB1R and

CB2R Ki = 1.37 nM) were obtained from the Department of Pharmacology and Toxicology (Virginia Commonwealth University, Richmond, VA). HIV-1 Tat_{1-101} was purchased from Immunodiagnostics (Woburn, MA). Stock solutions of Tat (10uM) were prepared in Sodium Citrate. Vehicle controls for Tat consisted of the same volume of sodium citrate that was used to dilute Tat in DMEM. Stock solutions of cannabinoids (10^{-2}M) were prepared in 100% ethanol and stored at -20°C. Stock solutions of cannabinoids were diluted in DMEM immediately before use to yield a final concentration of 10^{-6} M and ethanol concentration of 0.01%. Controls for cannabinoids consisted of equal volumes of ethanol.

Treatment of BV-2 Cells

BV-2 cells were seeded at a concentration of 10^6 cells/ well in serum-free media. They were then treated for 8h with sodium citrate buffer + vehicle (veh, 0.01% ethanol), Trans-Activator of Transcription (Tat) (50 nM) + veh, Tat (50 nM) + THC (10^{-6} M), or Tat (50 nM) + CP55940 (10^{-6} M) at 37ºC. After incubation time, the supernatant was collected and employed to assess cytokine/chemokine secretion through antibody membrane arrays (Bio Rad, Richmond, CA). Additionally, RNA was isolated and whole cell lysates were prepared for two dimensional electrophoresis.

Whole Cell Lysate and Protein Concentration

For analysis by 2-D gel electrophoresis, after treatment for 8h, cells were scraped from the bottom of the plate with PBS and were centrifuged (1000 rpm, 3 min). The

supernatant was collected and the cells were washed with PBS and centrifuged again (1000 rpm, 3 min). Thirty µl lysis buffer (7M urea, 2M thiourea, 4% CHAPS detergent, 30mM Tris buffer, 5nM magnesium acetate at pH 8.5) were added to each sample. Lysates were placed on ice for 30 min, sonicated (5X), and placed on ice for an additional 10 min. Samples were then centrifuged (12,000 xg, 10 min, 4ºC) and kept at -80ºC. Protein concentration was determined using the RC/DC protein kit (Bio Rad) according to the Lowry method (Lowry, 1951) by comparing samples to standard volumes of bovine albumin serum (BSA).

MTT Assay

The 3-(4,5-dimethyl-2-thiazolyl)-2,5-diphenyl-2H-tetrazolium bromide (MTT) assay was performed in order to ensure BV-2 cell viability with treatment. After 8 h treatment as described above, cell viability was measured by the reduction of MTT by viable mitochondria in a colorimetric assay described by Mosmann. (Mosmann, 1983). The absorbance was read with a SpectraMax 250 spectrophotometer (MDS Analytical Technologies) with a wavelength of 595 nm with a correction wavelength of 655 nm. The level of MTT reduction was expressed graphically as a percentage of that of the negative control (BV-2 cells in veh). Streptomycin was used as a positive control, since it induces apoptosis.

Two-Dimensional Gel Electrophoresis

The whole cell lysate (50ug) was combined with 300ul of rehydration buffer (Bio Rad) to hydrate a Readystrip 17 cm IPG strip (BioRad, pH 5-8) overnight according to manufacturer protocol. Mineral oil was added on top of the strip to prevent evaporation. IPG strips were subjected to electrofocusing for approximately 40,000 Volt-hours using the BioRad Protean IEF Cell unit. Strips then were stored at -80°C until used for second dimension electrophoresis. Before electrophoresis, strips were equilibrated for 15 min in both Equilibration Buffer I and II (BioRad). The second dimension was resolved in a 10% SDS-polyacrylamide gel using a BioRad power pac 1000 at a constant current constant of 40 mA. Gels were immediately preceded to Vorum silver stain that is compatible with Mass Spectrometry.

Vorum Silver Staining of Two-Dimensional Gels

Two-dimensional gels were subjected to Vorum silver staining as described by Lin et al (2008). Briefly, after gel electrophoresis, the gel was placed overnight in fixative consisting of 50% methanol, 12% acetic acid, and 0.05% formalin. The following day, the gel was washed three times (20 min each) with 35% ethanol. The gel then was washed twice (10 min each) with distilled water and sensitized (2 min) with 100mM sodium thiosulfate (Fisher) and 30mM potassium ferrocyanide (Amresco Solon, OH). The gel then was washed four times with water (4 min each). The gel then was treated (20 min) with 0.2% silver nitrate (Amresco) and 0.076% formalin. Following a wash (twice, 1 min each) with distilled water, the gel was developed (3-5 min) in a solution consisting of 6% sodium carbonate (VWR), 0.05% formalin, and 0.0004% sodium thiosulfate.

Development was terminated by immersion of the gel in a solution of 50% Methanol and 12% acetic acid for 5 min and washing in water for 10-15 min. Gels were scanned immediately after the water wash.

Analysis of Two-Dimensional Gels

Silver-stained gels were scanned using a ScanMaker 9800XL (Microtek) and analyzed using PDQuest version 8.0 differential analysis software (BioRad). Each treatment group was performed in triplicate, and using the spot-detection software, the density of spots was compared between replicate gels and between different experiments.

RayBio Mouse Cytokine Antibody Array

BV-2 cells (10^6 cells/ well) were treated for 8h with veh, Tat (50 nM) + veh, Tat (50 nM) + THC (10^{-6} M), or Tat (50 nM) + CP55940 (10^{-6} M) at 37ºC. After treatment of BV-2 cells, supernatants were subjected to a mouse cytokine antibody array 3 (RayBiotech, Inc., Norcross, GA.) according to the provided protocol in order to assess the levels of chemokines and cytokines in culture supernatants. Membranes from the 4 experimental groups were blocked in blocking buffer for 30 min at room temperature, and then were incubated overnight with supernatants from each of the four treatment groups at 4°C. Membranes were washed 3 times (5 min each) with Wash Buffer I and 2 times (5 min each) with Wash Buffer II and incubated with biotin-conjugated antibody for 2 h. Following the repetition of washes, membranes then were incubated with HRP-streptavidin (1:1,000) for 2 h. The membranes then were washed and developed by

chemiluminescence using the kit provided (250ul Detection Buffer C and 250ul Detection Buffer D) and exposed to Kodak BioMax XAR Film for 5 sec. The film was scanned on a Microtek ScanMaker 9800XL/TMA1600flatbed scanner (Microtek Lab Inc., Cerritos, CA). To determine relative concentration, the density of each spot was quantified and compared to standards using Quanti One software (BioRad).

RNA Isolation

BV-2 cells (10^6 cells/ well) were treated for 8h with veh, Tat (50 nM) + veh, Tat (50 nM) + THC (10^{-6} M), or Tat (50 nM) + CP55940 (10^{-6} M) at 37ºC. Total RNA was isolated from cells using TRIzol reagent (InvitrogenTM Life Technologies, Carlsbad, CA) according to the manufacturer's instructions. A chloroform-isopropanol extraction was performed, and the RNA was resuspended in 30µl sterile water. RNA cleanup was performed using a RNeasy Mini (Qiagen) kit according to the manufacturer's instructions. The 260 nm/280 nm ratio of RNA was taken to ensure integrity and the RNA was run on a 1.5% agarose gel and .

cDNA Synthesis and RT-PCR

Real-time Reverse Transcriptase-Polymerase Chain Reaction (RT-PCR) was used to assess the presence of mRNA of select cytokines and chemokines under varying experimental conditions. Messenger RNA (1µg) was used to generate cDNA. The cDNA synthesis was performed with a RT2 First Strand kit (Qiagen) according to manufacturer's instructions. RT-PCR was performed using iQ SYBR Green SuperMix (Bio Rad). Plates

were placed in the SmartCycler (Cepheid, Sunnyvale, CA), and PCR was performed using the following program 95°C, 15 min; 40 cycles of (95°C, 30 sec; 55°C, 30 sec; and 72°C, 30 sec. Resulting PCR products were determined using the threshold cycle (C_t) values for each of the genes on the array. The result was analyzed by the Qiagen website program and plotted as heat maps or bar graphs. Fold changes in gene expression were calculated using the $\Delta\Delta C_t$ method. Built-in RNA quality controls were also utilized to provide the relative levels of genomic DNA contamination and inhibitors of either the reverse transcription or the PCR itself. By examining the C_t value consistency for the housekeeping genes a normalization method was determined.

Results

BV-2 Cell Viability

Initial experiments were designed to determine the optimal concentration of cannabinoid to be used in BV-2 microglia-like cell cultures that did not elicit overt cytotoxic effects. Two approaches were employed to confirm cell viability: MTT assay and light microscopy. Because MTT reduction can only occur in metabolically active cells, the MTT assay determines mitochondrial activity, which relates to the total number of viable cells. The MTT assay employs the conversion of water-soluble MTT (3-(4,5-dimethylthiazol-2-yl)-2,5-diphenyltetrazolium bromide) to an insoluble formazan, which is then solubilized. The concentration then can be determined by measuring optical density. Any increase or decrease in formazan concentration represents correspondingly an increase or decrease in the number of viable cells. The MTT assay (**Figure 1**) demonstrated that after 8h of treatment, cells treated with 10^{-5} M THC and CP55940 were not viable, ($\leq$ 50% of cells in culture were viable). Cells treated with 10^{-6} M of THC exhibited approximately 70% viability and cells treated with 10^{-6} M CP55940 exhibited approximately 100% viability. Thus, the percentage viability of BV-2 cells was always greater for CP55940 versus THC regardless of what cannabinoid was employed in the presence of absence of Tat. These results were confirmed by light microscopy examination of cells maintained

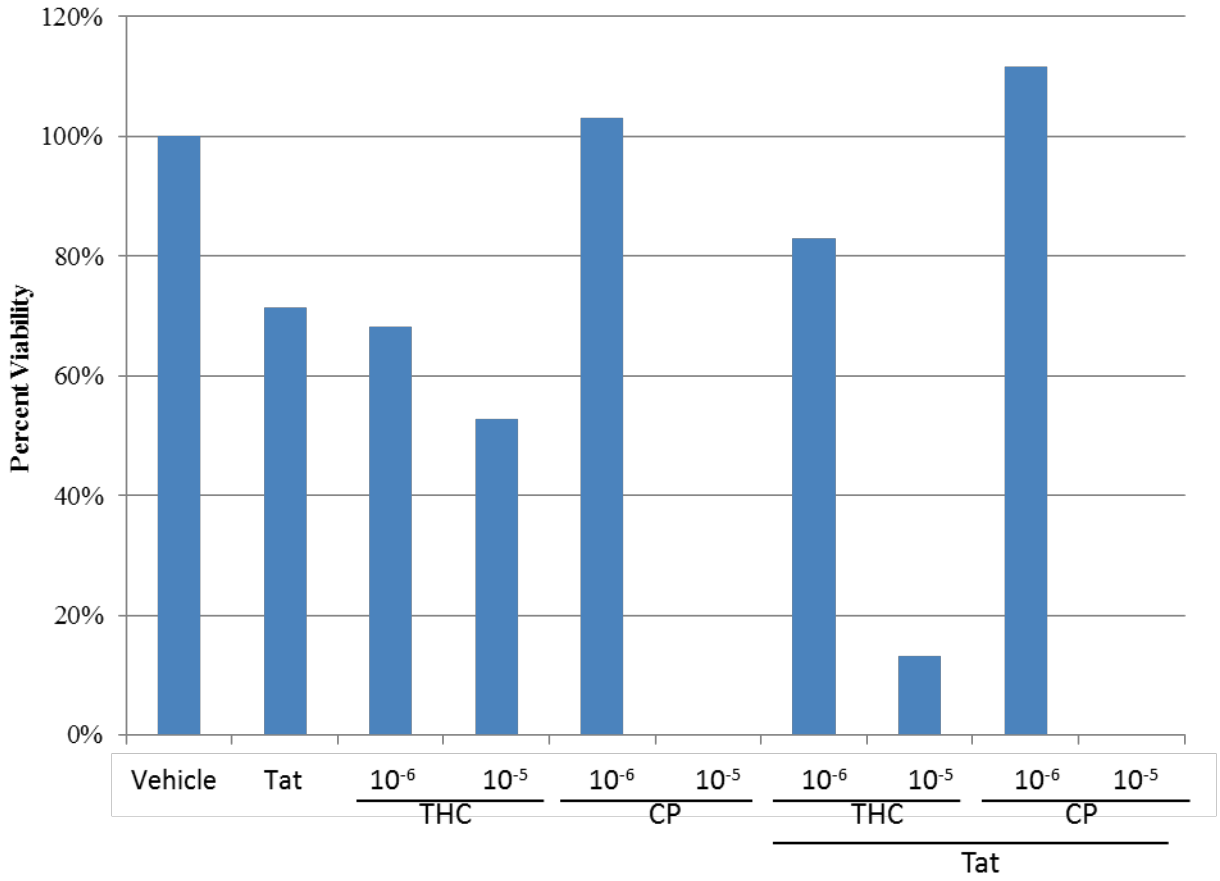

Figure 1. Viability of BV-2 Mouse Microgia-like Cells Treated with Varying Concentrations of HIV Protein Tat and Cannabinoids Measured by Hydrolysis of MTT by Mitochondria of Viable Cells. BV-2 cell cultures were treated (8h) with vehicle or cannabinoids (10^{-6} or 10^{-5}M) in the presence or absence of Tat (50nM). The graph represents percentage viability compared with that of cells maintained in vehicle consisting of sodium citrate and 0.01% ethanol in medium.

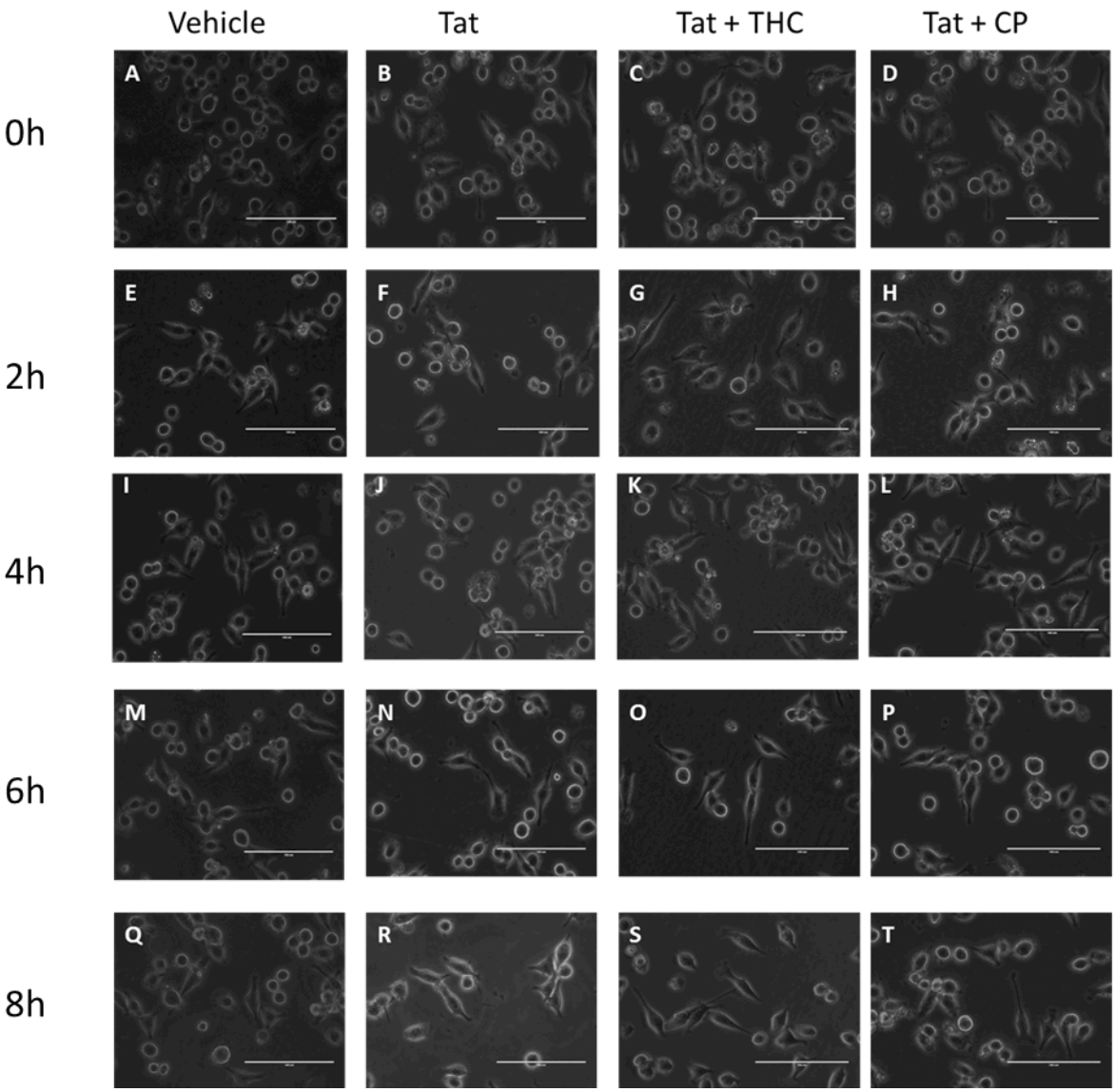

Figure 2. Light Microscopy of BV-2 Cells Exposed to Tat and Cannabinoids. BV-2 cells (10^6/well) were maintained in vehicle (0.01% ethanol), Tat (50nM) + vehicle, and cannabinoid THC or CP55940 (10^{-6}M) + Tat for the identified time periods. The bar in each panel represents 100μm.

for 8h in 10^{-6}M cannabinoid. BV-2 mouse microglial cells were examined before treatment (**Figure 2a-d)**, 2h post-treatment (**Figure 2e-h**), 4h post-treatment (**Figure 2i-l)**, 6h post-treatment (**Figure 2m-p)**, and 8h post-treatment (**Figure 2q-t)**. Cells maintained viability throughout this time course of examination. Consistent with the MTT assay data, treatment with 50nM Tat in the presence of cannabinoid 10^{-6} M did not alter cell shape or cell viability. Based on these collective results, an experimental model of 8h simultaneous treatment with 10^{-6}M and 50nM Tat was selected.

BV-2 Intracellular Protein Profile

A two dimensional (2-D) gel electrophoresis approach that combines isoelectric focusing with SDS-PAGE was employed for assessment of the BV-2 intracellular proteome. This approach was selected because it allows for the separation and quantification of a multiplicity of proteins on a single gel (O'Farrell, 1974). BV-2 cells were treated (8h) with vehicle (sodium citrate + 0.01% ethanol), Tat (50nM + 0.01% ethanol), Tat + THC (50nM Tat + 10^{-6}M THC), and Tat + CP55940 (50nM Tat + 10^{-6}M CP). Each group was run in triplicate. The results of a representative gel from each treatment group are shown in **Figure 3.** Each protein was identified as having a specific isoelectric point and molecular weight coordinate using PDQuest 8.0 software based on alignment of triplicate gels to create a master gel and alignment to match corresponding spots. Assessment of the master gel and analysis of the density of each spot allowed for

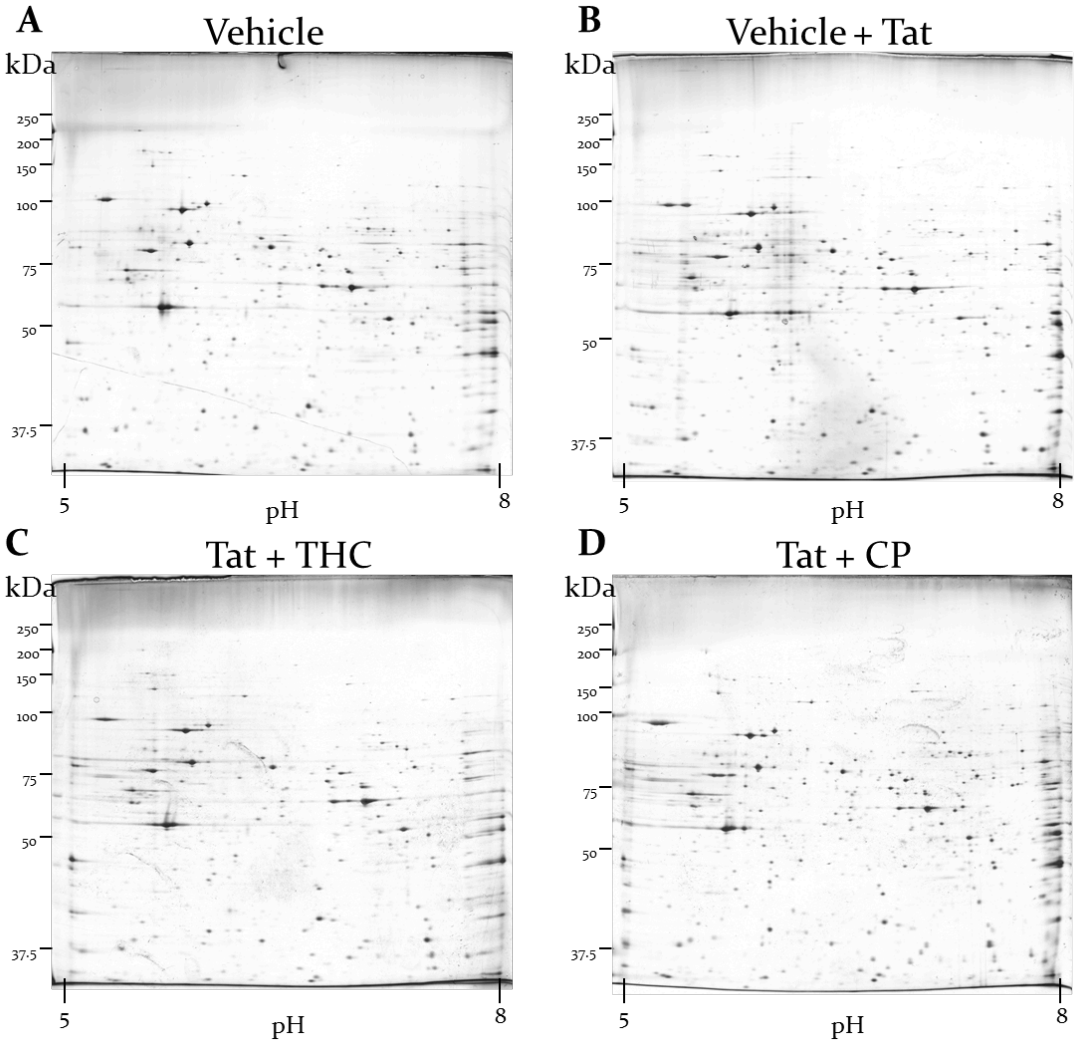

Figure 3. Two-Dimension Gel Protein Profiles of Whole Cell Homogenates of BV-2 cells treated with Tat and Cannabinoids. A representative Vorum silver stained gel from 3 separate experiments of BV-2 mouse microglia-like cells treated with 0.01% ethanol and sodium citrate (A), 50nM Tat + 0.01% ethanol (B), 50nM Tat + 10^{-6} M THC (C), and 50nM Tat + 10^{-6} M CP55940 (D). Samples shown were subjected to isoelectric focusing with 17 cm IPG Readistrips with a pH range of 5-8 and then were subjected to 10% SDS-PAGE in the second dimension. The horizontal axis represents protein separation by isoelectric focusing, while the vertical axis represents protein separation by relative molecular weight (kDa).

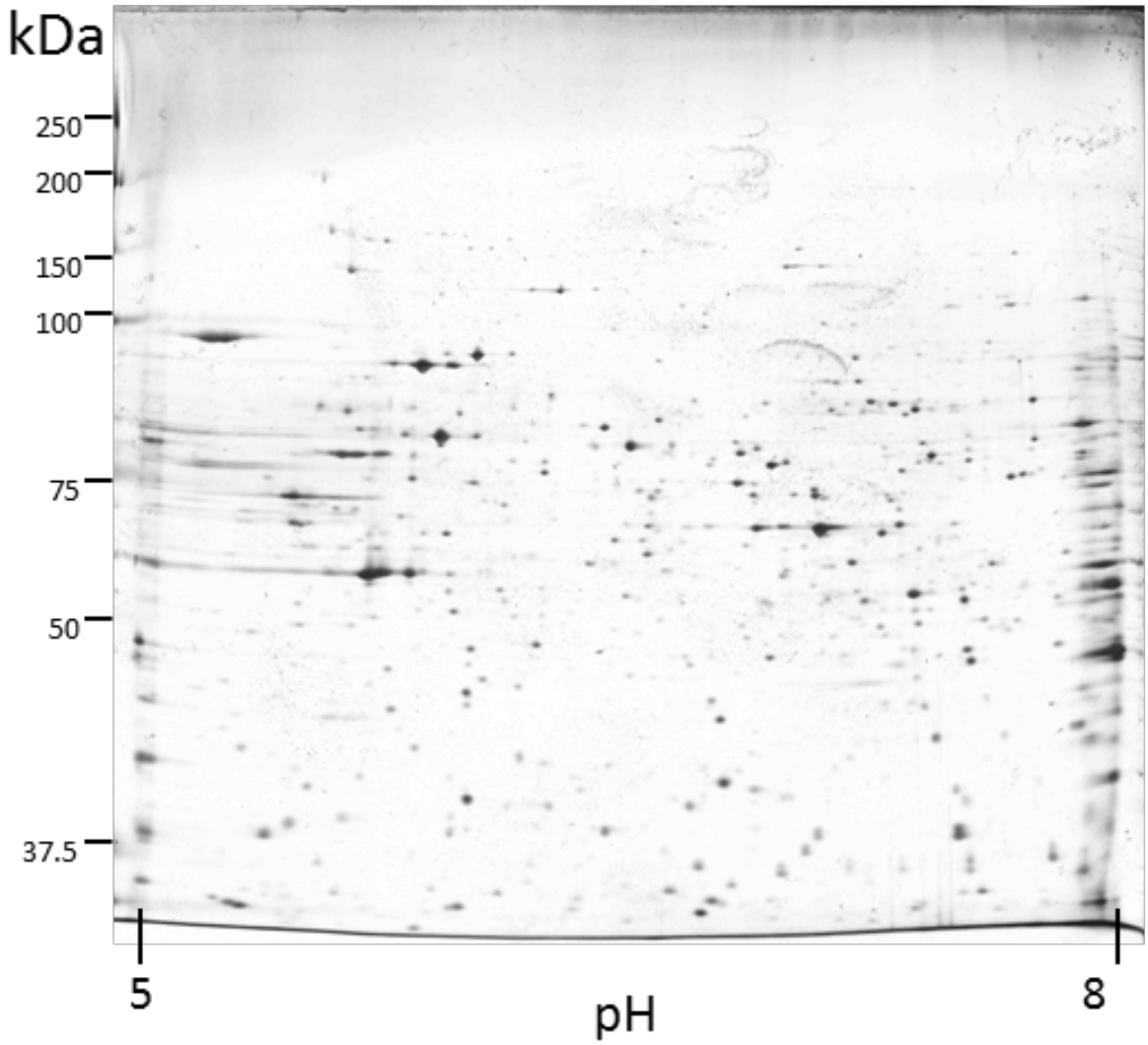

Figure 4. Representative Two-Dimensional Vorum-stained Gel Depicting Assessment of Coordinate Spot Identification Used for Establishing Scatterplot Analysis

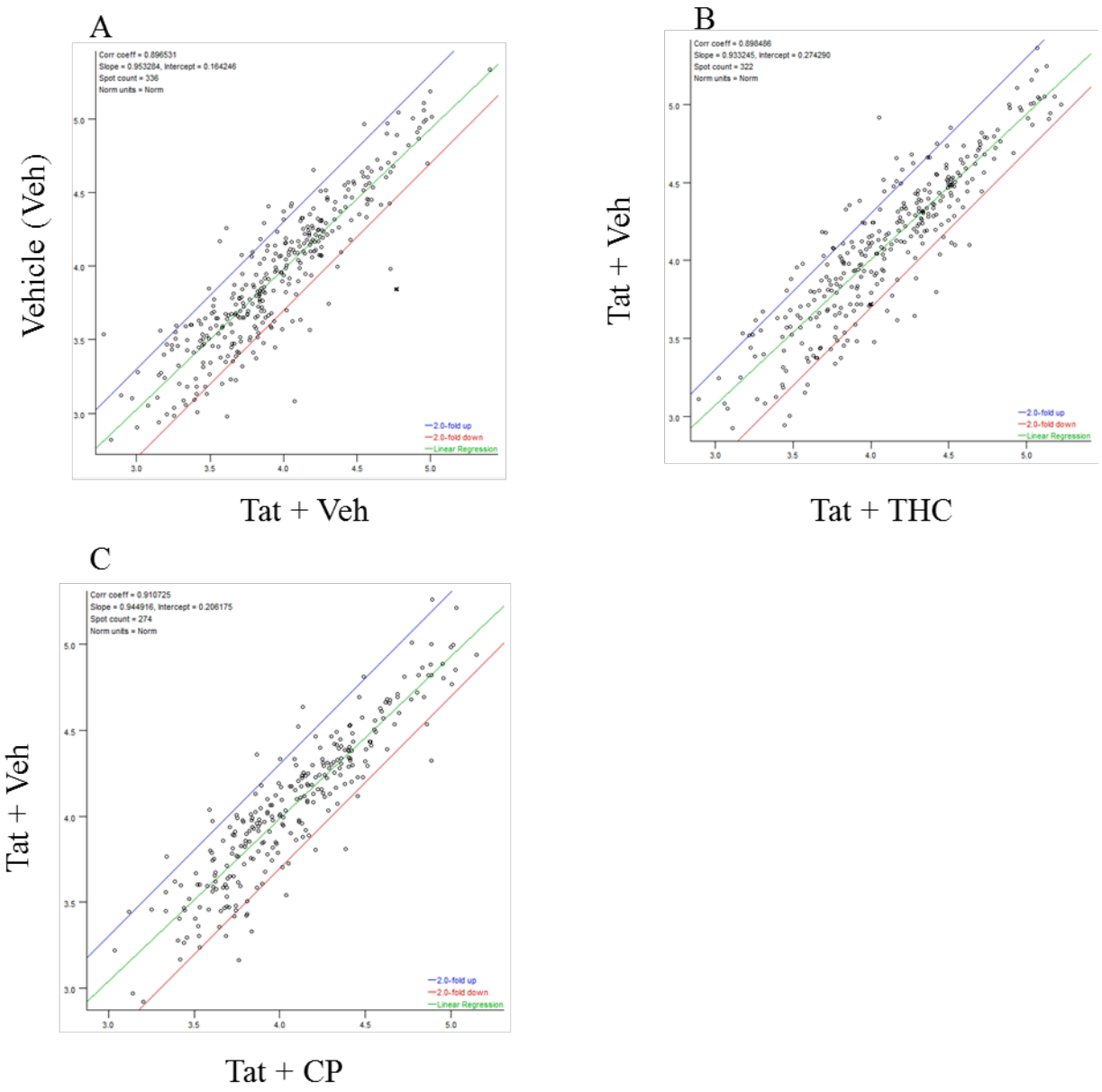

Figure 5. Scatterplot Spot Comparison Between Replicate Two-Dimensional Gels. PDQuest version 8.0 software was employed to identify, relative spot densities from each gel. Samples were analyzes in triplicate and subjected to comparison between treatment groups. The blue and red lines represent 2.0 standard deviation up-regulation and 2.0 standard deviation down-regulation, respectively.

the comparisons between group and the construction of scatter plots (**Figure 5**). A representative Vorum-stained gel that has been subjected to spot analysis is shown in **Figure 4.** Gels treated with vehicle as compared with gels treated with Tat had a total matched spot count of 336 with a correlation coefficient of 0.8965 (**Figure 5a)**. Gels treated with Tat and as compared with gels treated with Tat + THC shared 322 spots, with a correlation coefficient of 0.8985 (**Figure 5b)**. Gels treated with Tat as compared with gels treated with Tat + CP55940 shared 274 spots with a correlation coefficient of 0.9107 (**Figure 5c)**. In each graph, dots lying outside of the blue and red lines represent 2-fold higher level or 2-fold lower level of expression, respectively. Analysis of these gels indicated that there was a large degree of homology between the different treatment groups. While there were several individual proteins that showed a larger than 2-fold higher level or lower level with a given treatment, the majority of proteins exhibited no major differences in level, as least within the constraints of time, Tat, and cannabinoid exposure paradigm employed.

Cytokine and Chemokine Protein Profiles Secreted by BV-2 cells

Assessment of the BV-2 extracellular chemokine/cytokine profile was undertaken using a membrane array system (RayBiotech). Following 8h treatment, BV-2 cell supernatants were processed using the RayBiotech cytokine antibody array III (**Figure 6**). This experiment was done one time for proof of principle. Of the sixty-one proteins that can be detected using the system, twelve were selected for further analysis due to their change in expression between treatment groups: granulocyte colony-stimulating factor

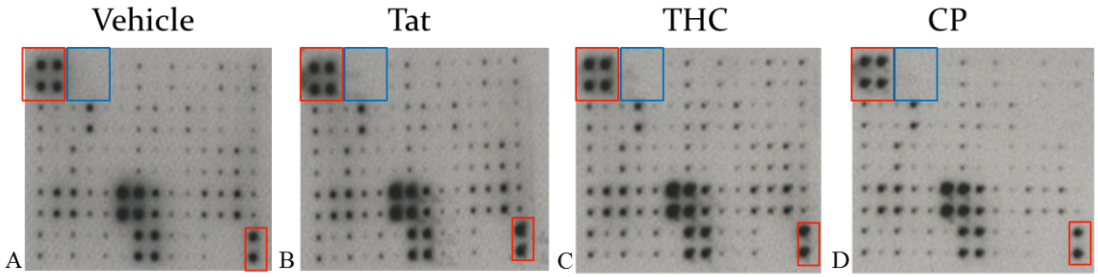

Pos	Pos	Neg	Neg	Blank	Axl	BCL	CD30L	CD30L	CD40	CRG-2	CTACK	CXCL16	Eotaxin
Pos	Pos	Neg	Neg	Blank	Axl	BCL	CD30L	CD30L	CD40	CRG-2	CTACK	CXCL16	Eotaxin
Eotaxin 2	Fas-ligand	Fractalkine	GCSF	GM-CSF	INF-γ	IGFBP-3	IGFBP-5	IGFBP-6	IL-1α	IL-1β	IL-2	IL-3	IL-3Rb
Eotaxin 2	Fas-ligand	Fractalkine	GCSF	GM-CSF	INF-γ	IGFBP-3	IGFBP-5	IGFBP-6	IL-1α	IL-1β	IL-2	IL-3	IL-3Rb
IL-4	IL-5	IL-6	IL-9	IL-10	IL-12	IL-12p70	IL-13	IL-17	KC	Leptin R	Leptin	LIX	L-Selectin
IL-4	IL-5	IL-6	IL-9	IL-10	IL-12	IL-12p70	IL-13	IL-17	KC	Leptin R	Leptin	LIX	L-Selectin
Lymphot.	MCP-1	MCP-5	M-CSF	MIG	MIP-1α	MIP-1γ	MIP 2	MIP 3β	MIP 3α	Pf 4	p-Selectin	RANTES	SCF
Lymphot.	MCP-1	MCP-5	M-CSF	MIG	MIP-1α	MIP-1γ	MIP 2	MIP 3β	MIP 3α	Pf 4	p-Selectin	RANTES	SCF
SDF-1α	TARC	TCA-3	TECK	TIMP-1	TNF- α	sTNFRI	sTNFRI	TPO	VCAM1	VERGF	Blank	Blank	Pos
SDF-1α	TARC	TCA-3	TECK	TIMP-1	TNF- α	sTNFRI	sTNFRI	TPO	VCAM1	VERGF	Blank	Blank	Pos

Figure 6. Effects the Cannabinoids THC and CP55940 on BV-2 Mouse Microglia-like Cell Extracellular Levels of Cytokines. Supernatants from BV-2 cells treated (8h) with 0.01% ethanol and sodium citrate (A), 50nM Tat + 0.01% ethanol (B), 50nM Tat + 10^{-6} M THC (C), and 50nM Tat + 10^{-6} M CP55940 (D) were subjected to RayBio Mouse Cytokine Array III. Red boxes indicate positive controls, while blue boxes indicate negative controls. Highlighted squares on the chart indicate cytokines and chemokines that were selected for further analysis.

(GCSF), insulin-like growth factor binding protein 3 (IGFBP-3), Interleukin 1 alpha (IL-1α), LPS-induced CXC chemokine (LIX/CXCL5), monocyte chemotactic protein 1 (MCP-1), monocyte chemotactic protein 5 (MCP-5), macrophage inflammatory protein 1 alpha (MIP-1α), macrophage inflammatory protein 1 gamma (MIP-1γ), macrophage inflammatory protein 2 (MIP-2), platelet factor 4 (PF-4), CCL5/RANTES, and soluble tumor necrosis factor receptor 1 (sTNFRI). These proteins were selected as they exhibited differential levels between treatment groups, as measured by intensity/mm^2 (**Table 1**). A graphical representation of these data is illustrated in **Figure 7**. Tat treatment resulted in an increase in level of select proteins. These data were also graphed according to fold change compared to treatment with vehicle (**Figure 8)**. As indicated by fold change, select cytokines, such as GCSF and LIX had no increase in expression when treated with Tat. They did, however, have decreased expression below baseline when treated with cannabinoids. Other chemokines, such as MIP-2, PF-4, MIPα, and RANTES showed an increase in level when treated with Tat. This increase was ablated when cells were treated with the cannabinoids THC or CP55940. In all cases, treatment with Tat and the cannabinoid CP55940 resulted in a decrease in expression below baseline levels of expression of cells subjected to no treatment.

Cytokine and Chemokine mRNA Profile by RT-PCR

In order to gain insight as to the site-of-action at which THC and CP55940 acted to diminish levels of established cytokine, RT-PCR was performed using a PCR array provided by SABiosciences (PAMM-011Z). Briefly, BV-2 cell whole homogenates were

	Treatment				
Cytokine	Vehicle	Tat	THC	CP	Classification
GCSF	107.1969	107.7232	96.06535	70.95646	Growth Factor
IGFBP-3	45.71497	58.35166	36.46535	37.94978	Binding Protein
IL-1α	106.9424	118.2773	77.18162	74.40868	Cytokine
LIX	69.90219	70.96045	52.84831	31.44696	CXC Chemokine
MCP1	408.2178	456.0289	334.7959	335.9918	CC Chemokine
MCP-5	169.3697	202.2650	201.5582	128.8688	CC Chemokine
MIP-1α	446.0233	564.6809	430.8201	342.1602	CC Chemokine
MIP-1γ	619.2085	674.2853	570.2347	565.0322	CC Chemokine
MIP-2	366.3371	484.0294	376.3764	328.9866	CXC Chemokine
PF-4	122.3430	193.9887	143.0114	104.9401	CXC Chemokine
RANTES	179.2407	264.3933	217.9427	163.9925	CC Chemokine
sTNF RI	436.9920	484.4102	464.0807	383.1344	Receptor

Table 1. Select Proteins Processed using the RayBiotech Cytokine Antibody Array III. Shown in this table are the differential levels of select proteins as measured by intensity/mm^2 when exposed to vehicle (sodium citrate +0.01% ethanol), Tat (50nM) + vehicle, Tat (50nM) + THC (10^{-6}M), and Tat + CP55940 (10^{-6}M).

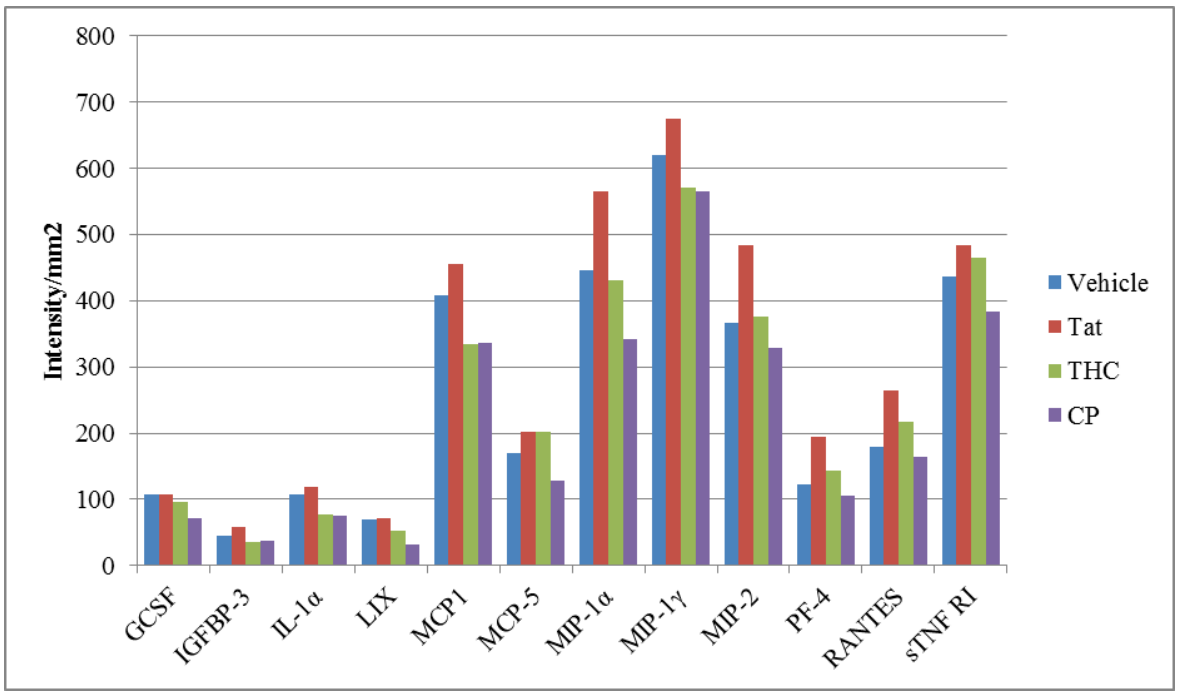

Figure 7. Relative Levels of Select Cytokines and Chemokines Present in Culture Supernatants of BV-2 Cells Treated with the HIV protein Tat in Concert with THC or CP55,940. Supernatants from BV-2 cells treated (8h) with 0.01% ethanol and sodium citrate, 50nM Tat + 0.01% ethanol, 50nM Tat + 10^{-6} M THC, or 50nM Tat + 10^{-6} M CP55940 were subjected to RayBio Mouse Cytokine Array III. The graph represents spots identified in the arrays and analyzed by densitometry.

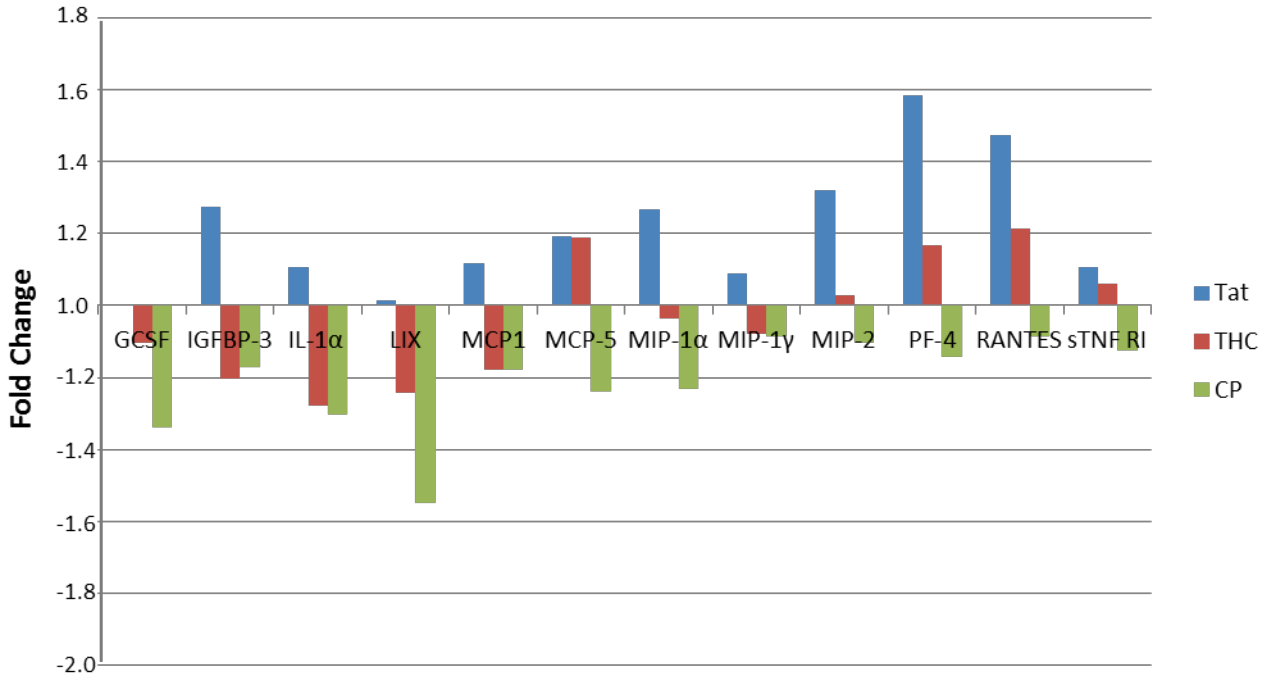

Figure 8. Relative Levels of Select Cytokines and Chemokines Present in Culture Supernatants of BV-2 Cells Treated with the HIV Protein Tat in Concert with THC or CP55,940. Supernatants from BV-2 cells treated for 8h with 0.01% ethanol and sodium citrate (A), 50nM Tat + 0.01% ethanol (B), 50nM Tat + 10^{-6} M THC (C), and 50nM Tat + 10^{-6} M CP55940 (D) were subjected to RayBio Mouse Cytokine Array III. Each protein concentration is representative as a fold change compared to treatment with vehicle.

subjected to total RNA isolation, RT-PCR, and assessment for inflammatory cytokine and chemokine mRNAs following 8h exposure to Tat ± cannabinoids or vehicle. Eighty-four inflammatory genes (**Figure 9**) were selected for assessment. Heat map comparisons were established between treatment groups (**Figures 10-12)**. Among the 84 genes, 11 were selected for further analysis: Ccl11, Ccl5, Ccl8, Ccr2, Ccr3, Ccr5, Cxcl1, Cxcr5, Il17f, Il5, and Tnfsf11. As shown in **Figure 13**, among these 11 genes, there was an increase in levels following exposure to the HIV inflammatory protein Tat. This increased level of expression was partially or fully ablated by co-exposure (8h) of cells to 10^{-6}M THC or CP55940.

Position	Symbol	Description	Gene Name
A01	Aimp1	Aminoacyl tRNA synthetase complex-interacting multifunctional protein 1	9830137A06Rik, AIMP1, p43, EMAPII, Emap2, Scye1, p43
A02	Bmp2	Bone morphogenetic protein 2	AI467020, Bmp2a
A03	Ccl1	Chemokine (C-C motif) ligand 1	BF534335, I-309, Scya1, Tca-3
A04	Ccl11	Chemokine (C-C motif) ligand 11	Scya11, eotaxin
A05	Ccl12	Chemokine (C-C motif) ligand 12	MCP-5, Scya12
A06	Ccl17	Chemokine (C-C motif) ligand 17	Abcd-2, Scya17, Scya17l, Tarc
A07	Ccl19	Chemokine (C-C motif) ligand 19	CKb11, ELC, MIP3B, Scya19, exodus-3
A08	Ccl2	Chemokine (C-C motif) ligand 2	AI323594, HC11, JE, MCAF, MCP-1, MCP1, SMC-CF, Scya2, Sigje
A09	Ccl20	Chemokine (C-C motif) ligand 20	CKb4, LARC, MIP-3A, MIP-3[a], MIP3A, ST38, Scya20, exodus-1
A10	Ccl22	Chemokine (C-C motif) ligand 22	ABCD-1, DCBCK, MDC, Scya22
A11	Ccl24	Chemokine (C-C motif) ligand 24	CKb-6, MPIF-2, Scya24
A12	Ccl3	Chemokine (C-C motif) ligand 3	AI323804, G0S19-1, LD78alpha, MIP-1alpha, MIP1-(a), MIP1-alpha, Mip1a, Scya3
B01	Ccl4	Chemokine (C-C motif) ligand 4	AT744.1, Act-2, MIP-1B, Mip1b, Scya4
B02	Ccl5	Chemokine (C-C motif) ligand 5	MuRantes, RANTES, SISd, Scya5, TCP228
B03	Ccl6	Chemokine (C-C motif) ligand 6	MRP-1, Scya6, c10
B04	Ccl7	Chemokine (C-C motif) ligand 7	MCP-3, Scya7, fic, marc, mcp3

B05	Ccl8	Chemokine (C-C motif) ligand 8	1810063B20Rik, AB023418, HC14, MCP-2, Mcp2, Scya8
B06	Ccl9	Chemokine (C-C motif) ligand 9	CCF18, MRP-2, Scya10, Scya9
B07	Ccr1	Chemokine (C-C motif) receptor 1	Cmkbr1, Mip-1a-R
B08	Ccr10	Chemokine (C-C motif) receptor 10	Cmkbr9, Gpr2, MGC151420
B09	Ccr2	Chemokine (C-C motif) receptor 2	Cc-ckr-2, Ccr2a, Ccr2b, Ckr2, Ckr2a, Ckr2b, Cmkbr2, mJe-r
B10	Ccr3	Chemokine (C-C motif) receptor 3	CC-CKR3, CKR3, Cmkbr1l2, Cmkbr3, MGC124265, MGC124266
B11	Ccr4	Chemokine (C-C motif) receptor 4	CHEMR1, Cmkbr4, LESTR, MGC151418, Sdf1r
B12	Ccr5	Chemokine (C-C motif) receptor 5	AM4-7, CD195, Cmkbr5
C01	Ccr6	Chemokine (C-C motif) receptor 6	CC-CKR-6, CCR-6, Cmkbr6, KY411
C02	Ccr8	Chemokine (C-C motif) receptor 8	Cmkbr8, MGC123958, MGC123959, mCCR8
C03	Cd40lg	CD40 ligand	CD154, CD40-L, Cd40l, HIGM1, IGM, IMD3, Ly-62, Ly62, T-BAM, TRAP, Tnfsf5, gp39
C04	Csf1	Colony stimulating factor 1 (macrophage)	C87615, Csfm, MCSF, op
C05	Csf2	Colony stimulating factor 2 (granulocyte-macrophage)	Csfgm, Gm-CSf, MGC151255, MGC151257, MGI-IGM
C06	Csf3	Colony stimulating factor 3 (granulocyte)	Csfg, G-CSF, MGI-IG
C07	Cx3cl1	Chemokine (C-X3-C motif) ligand 1	AB030188, ABCD-3, AI848747, CX3C, Cxc3, D8Bwg0439e, Scyd1
C08	Cxcl1	Chemokine (C-X-C motif) ligand 1	Fsp, Gro1, KC, Mgsa, N51, Scyb1, gro
C09	Cxcl10	Chemokine (C-X-C motif) ligand 10	C7, CRG-2, INP10, IP-10, IP10, Ifi10, Scyb10, gIP-10, mob-1
C10	Cxcl11	Chemokine (C-X-C motif) ligand 11	Cxc11, H174, I-tac, Ip9, Itac, Scyb11, Scyb9b, b-R1, betaR1
C11	Cxcl12	Chemokine (C-X-C motif) ligand 12	AI174028, Pbsf, Scyb12, Sdf1, Sdf1a, Sdf1b, Tlsf, Tlsfa, Tlsfb, Tpar1

C12	Cxcl13	Chemokine (C-X-C motif) ligand 13	4631412M08Rik, ANGIE2, Angie, BCA-1, BLC, BLR1L, Scyb13
D01	Cxcl15	Chemokine (C-X-C motif) ligand 15	Scyb15, lungkine, weche
D02	Cxcl5	Chemokine (C-X-C motif) ligand 5	AMCF-II, ENA-78, GCP-2, LIX, Scyb5, Scyb6
D03	Cxcl9	Chemokine (C-X-C motif) ligand 9	BB139920, CMK, Mig, MuMIG, Scyb9, crg-10
D04	Cxcr2	Chemokine (C-X-C motif) receptor 2	CD128, CDw128, Cmkar2, Gpcr16, IL-8Rh, IL-8rb, IL8RA, Il8rb, mIL-8RH
D05	Cxcr3	Chemokine (C-X-C motif) receptor 3	Cd183, Cmkar3
D06	Cxcr5	Chemokine (C-X-C motif) receptor 5	Blr1, CXC-R5, CXCR-5, Gpcr6, MDR15
D07	Fasl	Fas ligand (TNF superfamily, member 6)	APT1LG1, CD178, CD95-L, CD95L, Fas-L, Faslg, Tnfsf6, gld
D08	Ifng	Interferon gamma	IFN-g, Ifg
D09	Il10ra	Interleukin 10 receptor, alpha	AW553859, CDw210, CDw210a, Il10r, mIL-10R
D10	Il10rb	Interleukin 10 receptor, beta	6620401D04Rik, AI528744, CRF2-4, Crfb4, D16H21S58, D21S58h, IL-10R2, Il10r2
D11	Il11	Interleukin 11	IL-11
D12	Il13	Interleukin 13	Il-13
E01	Il15	Interleukin 15	AI503618
E02	Il16	Interleukin 16	KIAA4048, mKIAA4048
E03	Il17a	Interleukin 17A	Ctla-8, Ctla8, IL-17, IL-17A, Il17
E04	Il17b	Interleukin 17B	1110006O16Rik, 1700006N07Rik, Zcyto7
E05	Il17f	Interleukin 17F	C87042, IL-17F
E06	Il1a	Interleukin 1 alpha	Il-1a
E07	Il1b	Interleukin 1 beta	IL-1beta, Il-1b
E08	Il1r1	Interleukin 1 receptor, type I	CD121a, CD121b, IL-iR, Il1r-1, MGC129154
E09	Il1rn	Interleukin 1 receptor antagonist	F630041P17Rik, IL-1ra
E10	Il21	Interleukin 21	-
E11	Il27	Interleukin 27	IL-27, IL-27p28, Il30, p28
E12	Il2rb	Interleukin 2 receptor,	CD122, IL-15Rbeta, IL15Rbeta,

		beta chain	Il-2, 15Rbeta, Il-2Rbeta, MGC118674, p70
F01	Il2rg	Interleukin 2 receptor, gamma chain	CD132, [g]c, gamma(c), gc
F02	Il3	Interleukin 3	BPA, Csfmu, HCGF, Il-3, MCGF, PSF
F03	Il33	Interleukin 33	9230117N10Rik, Il-33, Il1f11, NF-HEV
F04	Il4	Interleukin 4	Il-4
F05	Il5	Interleukin 5	Il-5
F06	Il5ra	Interleukin 5 receptor, alpha	CD125, CDw125, Il5r
F07	Il6ra	Interleukin 6 receptor, alpha	CD126, IL-6R, Il6r, MGC30256
F08	Il6st	Interleukin 6 signal transducer	5133400A03Rik, AA389424, BB405851, CD130, D13Ertd699e, gp130
F09	Il7	Interleukin 7	A630026I06Rik, Il-7, MGC129342, hlb368
F10	Lta	Lymphotoxin A	LT, LT-[a], LT-alpha, LT[a], LTalpha, Ltx, MGC117668, TNF-beta, TNFSF1, Tnfb, Tnfsf1b, hlb382
F11	Ltb	Lymphotoxin B	AI662801, LTbeta, Tnfc, Tnfsf3, p33
F12	Mif	Macrophage migration inhibitory factor	GIF, Glif, MGC107654
G01	Nampt	Nicotinamide phosphoribosyltransferase	1110035O14Rik, AI314458, AI480535, NAmPRTase, Pbef, Pbef1, Visfatin
G02	Osm	Oncostatin M	OncoM
G03	Pf4	Platelet factor 4	Cxcl4, Scyb4
G04	Spp1	Secreted phosphoprotein 1	2AR, Apl-1, BNSP, BSPI, Bsp, ETA-1, Eta, OP, Opn, Opnl, Ric, Spp-1
G05	Tnf	Tumor necrosis factor	DIF, MGC151434, TNF-alpha, TNFSF2, TNFalpha, Tnfa, Tnfsf1a
G06	Tnfrsf11b	Tumor necrosis factor receptor superfamily, member 11b (osteoprotegerin)	OCIF, Opg, TR1

G07	Tnfsf10	Tumor necrosis factor (ligand) superfamily, member 10	A330042I21Rik, AI448571, APO-2L, Ly81, TL2, Trail
G08	Tnfsf11	Tumor necrosis factor (ligand) superfamily, member 11	Ly109l, ODF, OPG, OPGL, RANKL, Trance
G09	Tnfsf13	Tumor necrosis factor (ligand) superfamily, member 13	2310026N09Rik, April, MGC106105, Tall2, Trdl1
G10	Tnfsf13b	Tumor necrosis factor (ligand) superfamily, member 13b	BAFF, BLyS, D8Ertd387e, MGC124060, MGC124061, TALL-1, TALL1, THANK, TNFSF20, zTNF4
G11	Tnfsf4	Tumor necrosis factor (ligand) superfamily, member 4	Ath-1, Ath1, CD134L, OX-40L, Ox40l, TXGP1, Txgp1l, gp34
G12	Vegfa	Vascular endothelial growth factor A	Vegf, Vegf120, Vegf164, Vegf188, Vpf
H01	Actb	Actin, beta	Actx, E430023M04Rik, beta-actin
H02	B2m	Beta-2 microglobulin	Ly-m11, beta2-m, beta2m
H03	Gapdh	Glyceraldehyde-3-phosphate dehydrogenase	Gapd, MGC102544, MGC102546, MGC103190, MGC103191, MGC105239
H04	Gusb	Glucuronidase, beta	AI747421, Gur, Gus, Gus-r, Gus-s, Gus-t, Gus-u, Gut, asd, g
H05	Hsp90ab1	Heat shock protein 90 alpha (cytosolic), class B member 1	90kDa, AL022974, C81438, Hsp84, Hsp84-1, Hsp90, Hspcb, MGC115780
H06	MGDC	Mouse Genomic DNA Contamination	MIGX1B
H07	RTC	Reverse Transcription Control	RTC
H08	RTC	Reverse Transcription Control	RTC
H09	RTC	Reverse Transcription Control	RTC
H10	PPC	Positive PCR Control	PPC
H11	PPC	Positive PCR Control	PPC
H12	PPC	Positive PCR Control	PPC

Table 2. Topographical representation of the PCR Array Plate. The housekeeping genes were Ccl12, Csf1, Il6ra, and Gapdh.

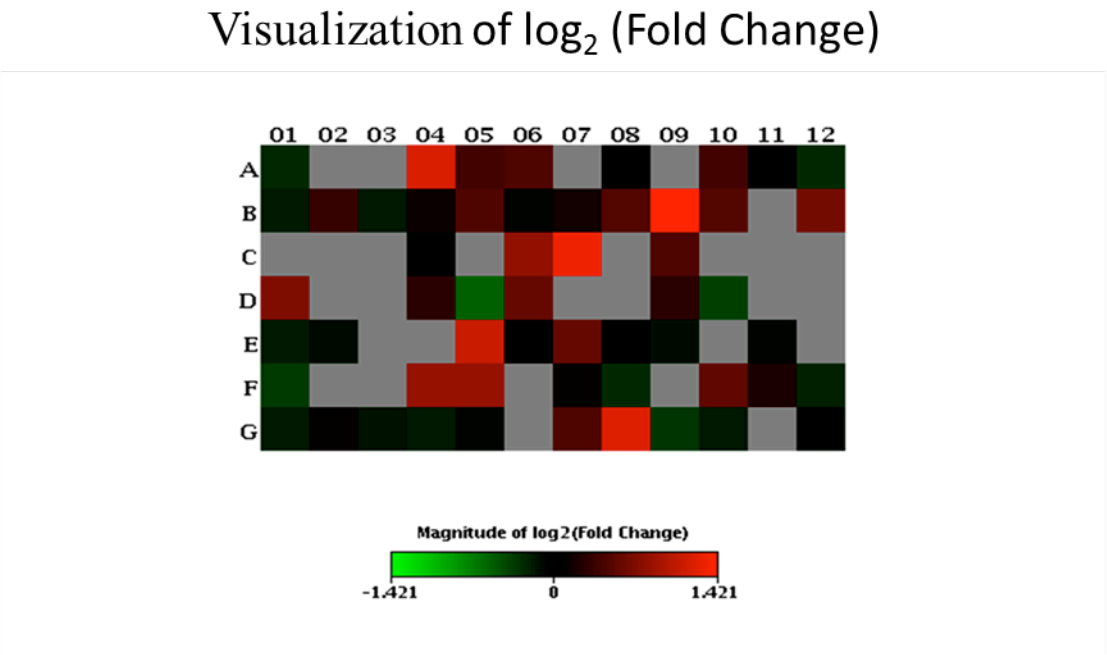

Figure 9. Heat Map Illustrating the Magnitude of Levels of Cytokines/Chemokines Maintained in Vehicle Versus Tat. BV-2 cells were treated (8h) with 0.01% ethanol and sodium citrate (vehicle) or 50nM Tat + 0.01% ethanol (Tat).

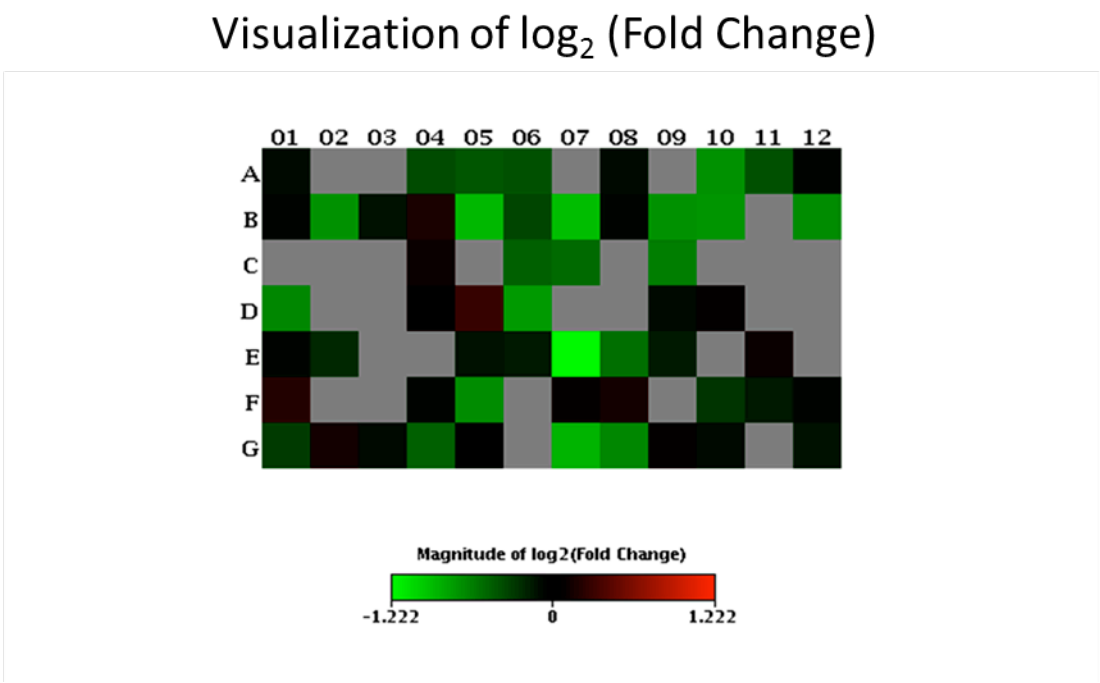

Figure 10. Heat Map Illustrating the Comparison of the Magnitude of Levels of Cytokine/Chemokine Maintained in Tat + vehicle versus Tat + THC. BV-2 cells were treated (8h) with 50nM Tat + 0.01% ethanol (Tat) and 50nM Tat + 10^{-6}M THC (Tat + THC).

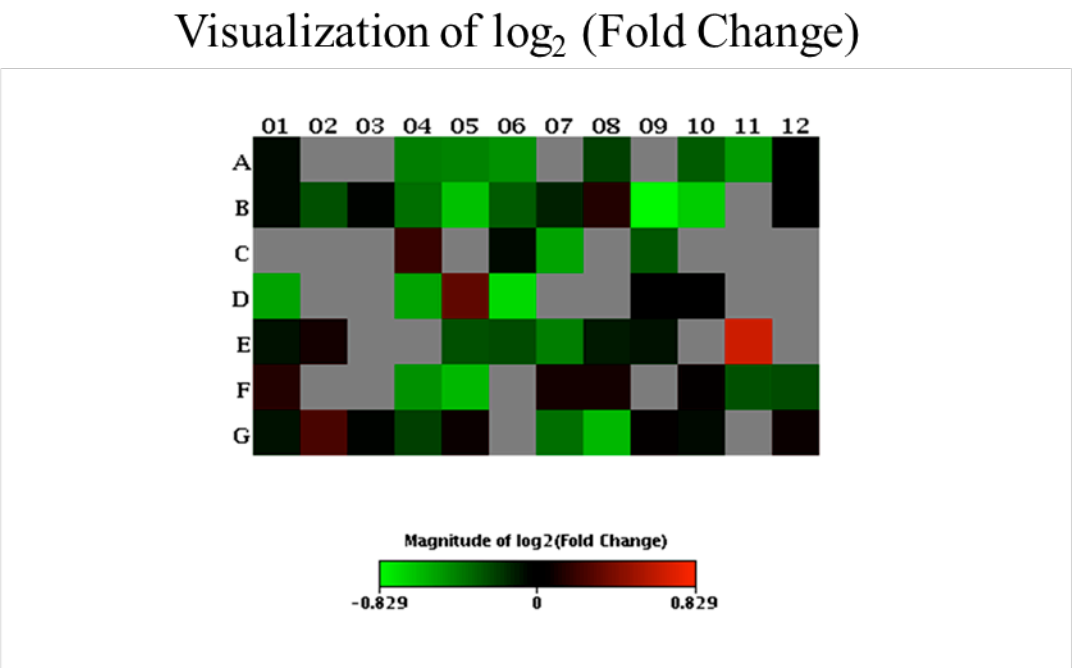

Figure 11. Heat Map Illustrating the Comparison of the Magnitude of Levels of Cytokine/Chemokine Maintained in Tat + Vehicle versus Tat + CP55940. BV-2 cells were treated (8h) with 50nM Tat + 0.01% ethanol (Tat) and 50nM Tat + 10^{-6}M CP55940 (Tat + CP).

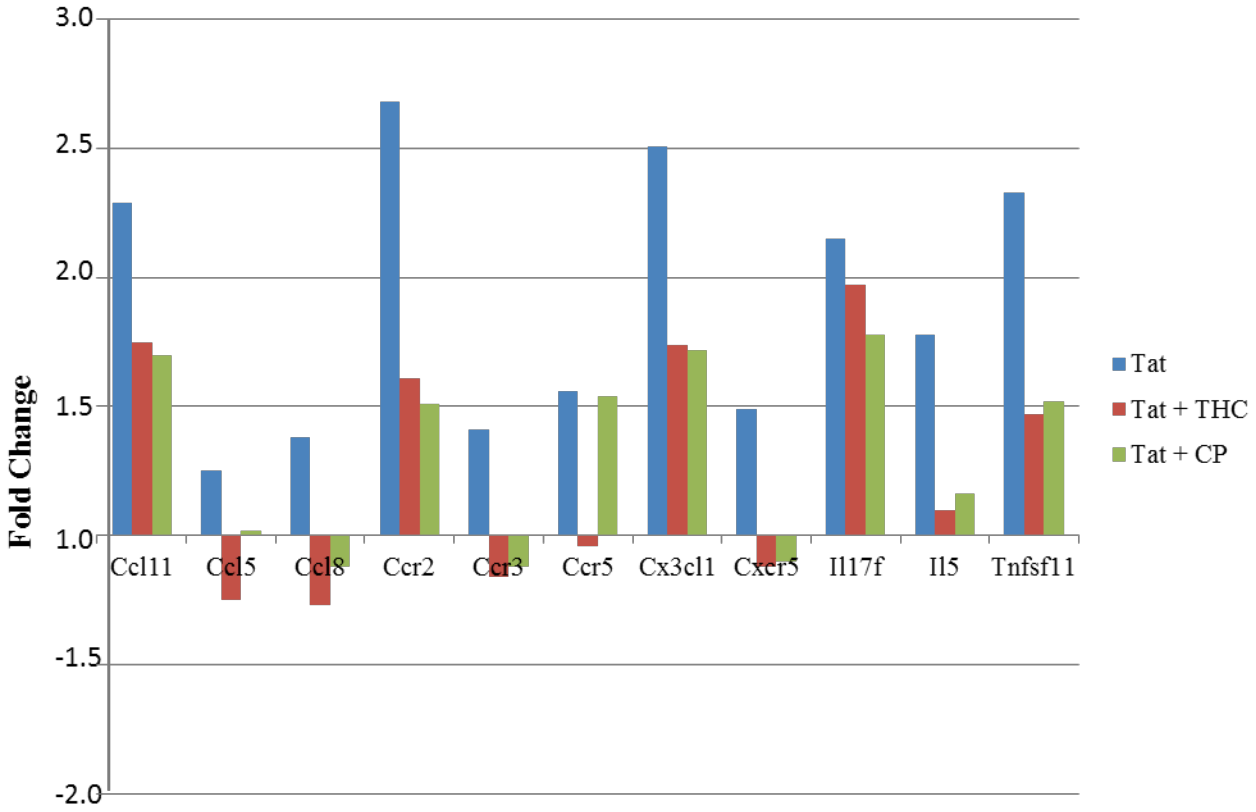

Figure 12. Gene Expression Profiles of Select Inflammatory Cytokines and Chemokines. Following 8h treatment of BV-2 cells with 0.01% ethanol and sodium citrate (vehicle), 50nM Tat + 0.01% ethanol (Tat), 50nM Tat + 10^{-6} M THC (Tat + THC), or 50nM Tat + 10^{-6} M CP55940 (Tat + CP), cells were subjected to quantitative RT-PCR array (PAMM-011Z; SABiosciences). Using web-based PCR array data analysis software provided by the manufacturer, fold-change compared to vehicle treatment was determined.

Discussion

The advent and widespread use of HAART has substantially increased the lifespan of patients infected with HIV-1 (Ances, 2008). With this increased life span is an increased chance to develop a myriad of HIV-associated neurocognitive disorders. In addition, most retroviral therapies utilize a combination of therapies of nucleoside analog reverse transcriptase inhibitors (NRTIs) and protease inhibitors (PIs). HIV pro-inflammatory protein Tat is not responsive to either of these actions and can therefore be responsible for inflammation in the brain. It is therefore imperative to develop methods of treatment that can combat this inflammation caused by HIV protein Tat.

According to a review by Cabral (2001), cannabinoids can alter immune cells at high concentrations (10^{-5}M or greater) by multiple modes of action, including physical disruption of membranes that could affect protein translational and post-translational events. Also, at high concentrations, due to its lipophilic nature, THC's interaction with cellular membranes could alter membrane fluidity, altering selective permeability (Wing, 1985). However, at low concentrations (less than 10^{-5}M) cannabinoids may affect immune cell function through activation of cannabinoid receptors. Cannabinoids may be ideal therapeutic agents due to their specificity of action, low cytotoxicity, selectivity, and

ability to cross the blood-brain barrier in nanomolar levels. While THC is only a partial agonist for the CB1R and CB2R, its use in experimental models yields insight regarding its drug abuse potential due to its deleterious psychoactive effects, and also gives valuable insight regarding specific molecular targets on immunocytes that have translational application.

Our interest in finding a therapeutic potential started at the protein level and was approached from a pharmacological perspective. Experiments were conducted to determine the effects of the cannabinoids THC and CP55940 on mouse microglial cells treated with Tat. Simultaneous treatment of Tat and THC or Tat and CP55940 was employed because pre-treatment with cannabinoids is not biologically relevant. The co-exposure rationale is to try to imitate more closely what occurs *in vivo,* and if a subject is already infected with HIV, he/she will already have the occurrence of Tat expression. In our experiments, BV-2 microglial-like cells were used. Although these cells are of mouse origin, they replicate most of the inflammatory responsiveness that has been attributed to human microglia in the context of HIV infection.

Within the constraints of the paradigm selected, there were no major effects on the BV-2 intracellular proteome between treatment groups. This was demonstrated using 2-D Gel Electrophoresis, which combines isoelectric focusing in the first dimension with with SDS-PAGE in the second dimension. This approach has high resolving capacity for a complex protein mixture and allowed for separation and quantification of proteins in a pH range of 5-8. There were no major changes in the proteome between treatment groups within the constraints of the experiment applied. However, it must be noted that analysis of

proteins occurred only within the range of pI 5 – 8 and it is possible that THC or CP55,940 could alter the expression levels of proteins beyond this range. For example, highly basic proteins would focus extending beyond a PI of 8, and the present methodology did not allow for their resolution. For example, the protocol applied to the present studies did not address whether THC or CP affected the expression of Tat-engendered proteins that could play a role in DNA binding or attaching to select DNA domains. A similar argument applies for proteins that would focus in the acid range (i.e., below a pI of 5). Nevertheless, the results indicate that the level of the majority of proteins elicited by Tat that were within the PI range of 5-8 were not affected in a major fashion by THC of CP55,940.

In contrast, there were overt effects on proteins that were secreted, as found by a microarray performed on supernatants of treated BV-2 cells. Analysis of a subset of proteins tested indicate that a majority of these proteins were chemokines. In addition, a subset of tested cytokines and chemokines displayed a differential gene expression profiles between treatment groups, as verified by RT-PCR analysis. While these experiments need to be repeated for statistical validity, these observations suggest that THC and CP act primarily by inhibiting the expression of chemokines, and that they do so by altering their level of transcription. However, the mechanism by which this is effected remains to be defined. That is, whether a cannabinoid receptor is linked functionally to these events awaits further analysis.

In summary, our findings are consistent with the hypothesis that select cannabinoids can ablate the pro-inflammatory response caused by HIV-1 pro-inflammatory protein Tat. However, due to time constraints, it was not possible to address whether these

cannabinoid-mediated effects were linked functionally to a cannabinoid receptor. A logical next step would be to perform Enzyme-linked immunosorbent assays (ELISAs) on select chemokines and cytokines that showed significant downregulation with cannabinoid treatment. Assessment of whether THC or CP cause a concentration-dependent inhibitory action suggestive of the involvement of a cannabinoid receptor, coupled with the appropriate use of receptor-selective cannabinoid receptor antagonists or anti-cannabinoid receptor mRNA siRNA technology, should provide insight as to whether a specified cannabinoid receptor subtype is involved. Ideally, if one were to avoid untoward psychoative properties that are associated with activation of the CB1R, a functional linkage would be found for the CB2R that is expressed on immune cells and is void of psychotropic action. Candidate chemokines for assessment include MIP-1α, MIP-2, PF-4, and RANTES as they showed the largest changes in secreted protein levels under experimental THC or CP exposure conditions.

Literature Cited

Literature Cited

1. Almeida OP, Lautenschlager NT. Dementia associated with infectious diseases. *Int Psychogeriatr*. 2005;17 Suppl 1:S65-77.

2. Ances BM, Clifford DB. HIV-associated neurocognitive disorders and the impact of combination antiretroviral therapies. *Curr Neurol Neurosci Rep*. 2008;8:455-461.

3. Benito C, Kim WK, Chavarria I, et al. A glial endogenous cannabinoid system is upregulated in the brains of macaques with simian immunodeficiency virus-induced encephalitis. *J Neurosci*. 2005;25:2530-2536.

4. Blasi E, Barluzzi R, Bocchini V, Mazzolla R, Bistoni F. Immortalization of murine microglial cells by a v-raf/v-myc carrying retrovirus. *J Neuroimmunol*. 1990;27:229-237.

5. Bornemann MA, Verhoef J, Peterson PK. Macrophages, cytokines, and HIV. *J Lab Clin Med*. 1997;129:10-16.

6. Bossi P, Dupin N, Coutellier A, et al. The Level of Human Immunodeficiency Virus (HIV) Type 1 RNA in Cerebrospinal Fluid As a Marker of HIV Encephalitis. *Clinical Infectious Diseases*. 1998;26:1072-1073.

7. Brigati C, Giacca M, Noonan DM, Albini A. HIV Tat, its TARgets and the control of viral gene expression. *FEMS Microbiol Lett*. 2003;220:57-65.

8. Cabral GA. Marijuana and Cannabinoids: Effects on Infections, Immunity, and AIDS. *J Cannabis Ther* 2001(3/4): 061-85.

9. Cabral GA, Staab A. Effects on the immune system. *Handb Exp Pharmacol*. 2005;(168):385-423.

10. Cabral GA, Dove Pettit DA. Drugs and immunity: cannabinoids and their role in decreased resistance to infectious disease. *J Neuroimmunol*. 1998;83:116-123.

11. Carter CA, Ehrlich LS. Cell biology of HIV-1 infection of macrophages. *Annu Rev Microbiol*. 2008;62:425-443.

12. Chang HK, Gallo RC, Ensoli B. Regulation of Cellular Gene Expression and Function by the Human Immunodeficiency Virus Type 1 Tat Protein. *J Biomed Sci*. 1995;2:189-202.

13. Chen P, Mayne M, Power C, Nath A. The Tat protein of HIV-1 induces tumor necrosis factor-alpha production. Implications for HIV-1-associated neurological diseases. *J Biol Chem*. 1997;272:22385-22388.

14. Compton DR, Gold LH, Ward SJ, Balster RL, Martin BR. Aminoalkylindole analogs: cannabimimetic activity of a class of compounds structurally distinct from delta 9-tetrahydrocannabinol. *J Pharmacol Exp Ther*. 1992;263:1118-1126.

15. D'Aversa TG, Yu KO, Berman JW. Expression of chemokines by human fetal microglia after treatment with the human immunodeficiency virus type 1 protein Tat. *J Neurovirol*. 2004;10:86-97.

16. Davis LE, Hjelle BL, Miller VE, et al. Early viral brain invasion in iatrogenic human immunodeficiency virus infection. *Neurology*. 1992;42:1736-1739.

17. Dayton AI, Sodroski JG, Rosen CA, Goh WC, Haseltine WA. The trans-activator gene of the human T cell lymphotropic virus type III is required for replication. *Cell*. 1986;44:941-947.

18. De Chiara G, Marcocci ME, Sgarbanti R, et al. Infectious agents and neurodegeneration. *Mol Neurobiol*. 2012;46:614-638.

19. Demarchi F, d'Adda di Fagagna F, Falaschi A, Giacca M. Activation of transcription factor NF-kappaB by the Tat protein of human immunodeficiency virus type 1. *J Virol*. 1996;70:4427-4437.

20. Dewey WL. Cannabinoid pharmacology. *Pharmacol Rev*. 1986;38:151-178.

21. Gartner S. HIV Infection and Dementia. *Science*. 2000;287:602-604.

22. Gaoni, Y and Mechoulam R. Isolation, Structure, and Partial Synthesis of an Active Constituent of Hashish. - *J Am Chem Soc.* - American Chemical Society;1964. :1646-1647.

23. Ghafouri M, Amini S, Khalili K, Sawaya BE. HIV-1 associated dementia: symptoms and causes. *Retrovirology*. 2006;3:28.

24. Gonzalez-Scarano F, Martin-Garcia J. The neuropathogenesis of AIDS. *Nat Rev Immunol*. 2005;5:69-81.

25. Henn A, Lund S, Hedtjarn M, Schrattenholz A, Porzgen P, Leist M. The suitability of BV2 cells as alternative model system for primary microglia cultures or for animal experiments examining brain inflammation. *ALTEX*. 2009;26:83-94.

26. Howlett AC. Cannabinoid receptor signaling. *Handb Exp Pharmacol*. 2005;(168):53-79.

27. Hudson L, Liu J, Nath A, et al. Detection of the human immunodeficiency virus regulatory protein tat in CNS tissues. *J Neurovirol*. 2000;6:145-155.

28. Lipton SA, Gendelman HE. Dementia Associated with the Acquired Immunodeficiency Syndrome. *N Engl J Med*. 1995;332:934-940.

29. Lowry OH, Rosebrough NJ, Farr AL, Randall RJ. PROTEIN MEASUREMENT WITH THE FOLIN PHENOL REAGENT. *Journal of Biological Chemistry*. 1951;193:265-275.

30. Lund S, Porzgen P, Mortensen AL, et al. Inhibition of microglial inflammation by the MLK inhibitor CEP-1347. *J Neurochem*. 2005;92:1439-1451.

31. McArthur JC, Becker PS, Parisi JE, et al. Neuropathological changes in early HIV-1 dementia. *Ann Neurol*. 1989;26:681-684.

32. McArthur JC, Brew BJ, Nath A. Neurological complications of HIV infection. *The Lancet Neurology*. 2005;4:543-555.

33. Mosmann T. Rapid colorimetric assay for cellular growth and survival: application to proliferation and cytotoxicity assays. *J Immunol Methods*. 1983;65:55-63.

34. Munro S, Thomas KL, Abu-Shaar M. Molecular characterization of a peripheral receptor for cannabinoids. *Nature*. 1993;365:61-65.

35. Navia BA, Jordan BD, Price RW. The AIDS dementia complex: I. Clinical features. *Ann Neurol*. 1986;19:517-524.

36. O'Farrell PH. High resolution two-dimensional electrophoresis of proteins. *Journal of Biological Chemistry*. 1975;250:4007-4021.

37. Peluso R, Haase A, Stowring L, Edwards M, Ventura P. A Trojan Horse mechanism for the spread of visna virus in monocytes. *Virology*. 1985;147:231-236.

38. Pertwee RG. Pharmacology of cannabinoid CB1 and CB2 receptors. *Pharmacol Ther*. 1997;74:129-180.

39. Pu H, Tian J, Flora G, et al. HIV-1 Tat protein upregulates inflammatory mediators and induces monocyte invasion into the brain. *Mol Cell Neurosci*. 2003;24:224-237.

40. Pugliese A, Vidotto V, Beltramo T, Petrini S, Torre D. A review of HIV-1 Tat protein biological effects. *Cell Biochem Funct*. 2005;23:223-227.

41. Ramirez SH, Sanchez JF, Dimitri CA, Gelbard HA, Dewhurst S, Maggirwar SB. Neurotrophins prevent HIV Tat-induced neuronal apoptosis via a nuclear factor-kappaB (NF-kappaB)-dependent mechanism. *J Neurochem*. 2001;78:874-889.

42. Wang T, Rumbaugh JA, Nath A. Viruses and the brain: from inflammation to dementia. *Clin Sci (Lond)*. 2006;110:393-407.

43. Wing, D. R., J. T. A. Leuschner, G. A. Brent, D. J. Harvey, and W. D. M. Paton. 1985. Quantification of *in vivo* membrane associated delta-9-tetrahydrocannabinol and its effects on membrane fluidity. *Proceedings of the 9th International Congress of Pharmacology 3rd satellite symposium on cannabis.* Harvey, D. J. Oxford: IRL Press.

VITA

Rebecca Anne Maddux was born on June 25, 1988 in Richmond, Virginia and is a citizen of the United States of America. She graduated from Midlothian High School, Midlothian, Virginia in 2006. She received a Bachelor of Science degree in Biology and a Bachelor of Arts degree in Spanish from the University of Virginia in 2010. Rebecca is continuing her education in medical school as part of the Virginia Commonwealth University School of Medicine class of 2017.